Solar Phys (2017) 292:181
DOI 10.1007/s11207-017-1207-z

Prediction of the Length of Upcoming Solar Cycles

Bharati Kakad[1,2] **· Amar Kakad**[1] **· Durbha Sai Ramesh**[1]

Received: 29 August 2017 / Accepted: 13 November 2017 / Published online: 24 November 2017

Abstract The forecast of solar cycle (SC) characteristics is crucial particularly for several space-based missions. In the present study, we propose a new model for predicting the length of the SC. The model uses the information of the width of an autocorrelation function that is derived from the daily sunspot data for each SC. We tested the model on Versions 1 and 2 of the daily international sunspot number data for SCs 10 – 24. We found that the autocorrelation width A_{w}^{n} of SC n during the second half of its ascending phase correlates well with the modified length that is defined as $T_{\mathrm{cy}}^{n+2} - T_{\mathrm{a}}^{n}$. Here T_{cy}^{n+2} and T_{a}^{n} are the length and ascent time of SCs $n+2$ and n, respectively. The estimated correlation coefficient between the model parameters is 0.93 (0.91) for Version 1 (Version 2) sunspot series. The standard errors in the observed and predicted lengths of the SCs for Version 1 and Version 2 data are 0.38 and 0.44 years, respectively. The advantage of the proposed model is that the predictions of the length of the upcoming two SCs (*i.e.*, $n+1$, $n+2$) are readily available at the time of the peak of SC n. The present model gives a forecast of 11.01, 10.52, and 11.91 years (11.01, 12.20, and 11.68 years) for the length of SCs 24, 25, and 26, respectively, for Version 1 (Version 2).

Keywords Solar cycle · Sunspots · Models

1. Introduction

The Sun is the energy source for our planet Earth. Variations in solar outputs (energetic particles, radiations, *etc.*) with both short and long timescales have significant effects on

✉ B. Kakad
bkakad9@gmail.com

A. Kakad
amar.kakad@gmail.com

D.S. Ramesh
dsramesh@iigs.iigm.res.in

[1] Indian Institute of Geomagnetism, Plot 5, Sector 18, New Panel (W), Navi Mumbai, 410218, Maharashtra, India

[2] Research Institute for Sustainable Humanosphere, Kyoto University, Uji, Kyoto 6110011, Japan

our life, on the near-Earth environment, and on modern space-based technology (McComas *et al.*, 2008; Emmert, Lean, and Picone, 2010; de Toma *et al.*, 2010; Ermolli *et al.*, 2013; Solomon, Qian, and Burns, 2013; Hajra *et al.*, 2014; Hao *et al.*, 2014). Periods of low solar activity like the Maunder and Dalton minimum have been witnessed in the past. Some studies also support the existence of grand minima in solar activity (Usoskin, Solanki, and Kovaltsov, 2011). The most evident solar variability is linked with the periodicity of 9 – 13.6 years, which is widely known as the solar cycle (SC). Realizing this fact, we are keen to know the nature of future solar activity. Today, different models are available with which to forecast the peak of an SC (Ohl, 1966; Feynman, 1982; Wilson, 1990; Thompson, 1993; Hathaway and Wilson, 2006; Muñoz-Jaramillo *et al.*, 2013; Svalgaard and Kamide, 2012). In spite of the availability of several models, each forecast possesses uncertainties, and hence their usage is sometimes questionable (Pesnell, 2008, 2016).

In addition to the peak solar activity, we are also interested to know the length of an upcoming SC. The extended minimum of SC 24 resulted in the third longest SC with a length of 12.5 years for SC 23. In the past, SCs 4 and 6 had greater lengths of 13.58 and 13.08 years, respectively, and it falls into the Maunder minimum period. The length and peak of the SC vary from one SC to another, which is physically related to the process of the solar dynamo (Dikpati and Gilman, 2008). Studies have suggested that a stronger SC is likely to have a shorter ascent time (Waldmeier, 1935, 1939). This dependence is widely known as the Waldmeier effect. In addition, the peak sunspot activity is found to be inversely correlated with the length of the preceding SC (Hathaway, Wilson, and Reichmann, 2002; Kane, 2008), which is known as an amplitude-period effect. This indicates that the length of the SC can give us some clue about the forthcoming solar activity. To date, there is no exclusive model for the prediction of the length of an SC. Recently Kakad, Kakad, and Ramesh (2015) proposed a new model solely for the prediction of the descent time of an SC; this model is based on the Shannon-Entropy technique.

In the present study, we have developed a new model for forecasting the length of an SC. This model uses the daily international sunspot number data (Versions 1 and 2) for SCs 10 – 23. The method we adopted to construct the model is described in Section 2. The results are discussed and concluded in Section 3.

2. Method for the Model Development

In the present study, we have used Versions 1 and 2 of the daily and monthly smoothed international sunspot number observations, which are available at http://www.sidc.be/silso/. In 2015, the original (*i.e.* Version 1) sunspot number series was replaced by the new series (*i.e.* Version 2). Several corrections were applied to these long-term sunspot data in order to remove inhomogeneities in past observations (Clette *et al.*, 2015, 2016b). This new sunspot number, Version 2 data, is now used by solar scientists. Many studies have recently been carried out using the new sunspot time series to validate previously proposed forecasting models (Zachilas and Gkana, 2015; Clette *et al.*, 2016a). In the present study, our aim is to develop a new model for the prediction of the length of an upcoming SC. This model is developed for Versions 1 and 2 of the sunspot data, which are depicted in Figure 1a and 1b, respectively. The solid black and yellow lines shown in Figure 1 represent the monthly smooth sunspot number (SSN) for the respective sunspot numbers.

Before we proceed to describe the model development, it is important to estimate the characteristics of SCs for the two sunspot number series. Using the monthly SSN, we computed the ascent time (T_{a}), descent time (T_{d}), length (T_{cy}), maximum sunspot number ($S_{\max}$),

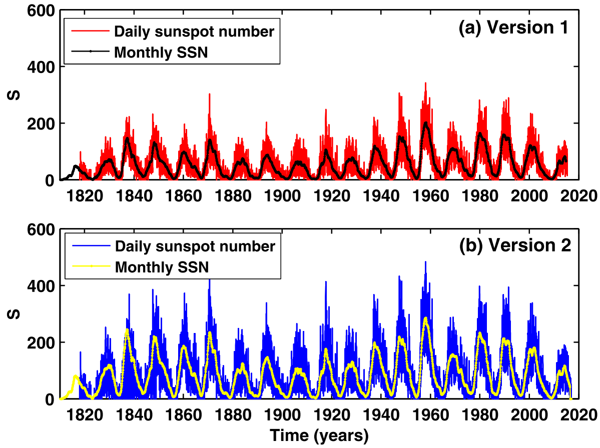

Figure 1 Variation in daily international sunspot number data (**a**) Version 1 (1 January 1818 to 31 May 2015) and (**b**) Version 2 (1 January 1818 to 31 December 2016). The monthly SSN is shown with the *solid dotted line* in the plots.

and minimum sunspot number (S_{min}) for each SC in the Version 1 and Version 2 data series. To obtain these characteristics, we identified the start time (t_{s}), peak time (t_{p}), and end time (t_{e}) for each SC. We identified the mathematical minimum and maximum in the monthly SSN for a given SC, and assigned their occurrence to the time of the start and peak, respectively. In addition to the mathematical maximum/minimum, different methods can be adopted to retrieve the SC characteristics (Hathaway, 2010). As SC characteristics obtained from different methods vary only slightly (Kakad, 2011), we decided to use the method based on the first occurrence of the mathematical minimum/maximum in the monthly SSN to obtain the SC characteristics.

The characteristics of the SC n were evaluated by the ascent time $T_{\mathrm{a}}^n = t_{\mathrm{p}}^n - t_{\mathrm{s}}^n$, the descent time $T_{\mathrm{d}}^n = t_{\mathrm{e}}^n - t_{\mathrm{p}}^n$, and the length $T_{\mathrm{cy}}^n = T_{\mathrm{a}}^n + T_{\mathrm{d}}^n$. The monthly SSNs at the time of t_{p}^n and t_{s}^n are represented by S_{max}^n and S_{min}^n , respectively, for SC n. The SC characteristics for the Version 1 and Version 2 data are compiled in Tables 1 and 2, respectively, for SCs 1 – 24. In Figure 2 we compare these characteristics for the Version 1 and Version 2 sunspot series. It is observed that the ascent time and descent time of the SCs are in good agreement for Versions 1 and 2, except for SCs 22 and 23. However, the length of SCs 1 – 24 are nearly the same for the Version 1 and Version 2 sunspot series, with a standard rms difference of 0.6 months. The difference in ascent and descent times of SCs 22 and 23 for the Version 1 and Version 2 sunspot series arises from the change in the peak time. Values of SC maximum (S_{max}) and minimum (S_{min}) are somewhat higher for Version 2 than for Version 1. S_{max} for Versions 1 and 2 follows similar trends in their variations, resulting in a good correlation (≈ 0.96) between them. Similarly, S_{min} for Versions 1 and 2 is also found to be in good correlation (≈ 0.97).

As stated earlier, in this model we used the daily international sunspot numbers. There are large data gaps in the daily sunspot numbers before 1855, so we used the sunspot data from SCs 10 – 24 in the present model. As a first step, we smoothed the daily sunspot data by taking three-day averages centered on a given day. For each jth day, this is represented by $S_{\mathrm{a}}(j)$. This three-day smoothing was applied to remove any sudden spikes in the sunspot time series and was used for further processing. We later divided the ascent phase of each SC into two equal parts and termed them Phases 1 and 2. For SC n, Phase 1 starts at t_{s}^n and ends at $t_{\mathrm{s}}^n + T_{\mathrm{a}}^n/2$, while Phase 2 starts at $t_{\mathrm{s}}^n + T_{\mathrm{a}}^n/2$ and ends at t_{p}^n.

Furthermore, we obtained $S_{\mathrm{a}} - \langle S_{\mathrm{a}} \rangle$ during Phase 2 of each SC and treated it as a signal to retrieve the autocorrelation function for the corresponding SC. The average of S_{a} during

Table 1 Solar cycle characteristics such as start time (t_s), peak time (t_p), ascent time (T_a), descent time (T_d), length of SC (T_{cy}), peak sunspot number (S_{max}), and minimum sunspot number (S_{min}) for the Version 1 sunspot series. The autocorrelation width (A_w), the length of SCs predicted using the model equation, and the error (τ_{error}) in the observed and predicted T_{cy} are given in the last three columns.

SC No.	Start time t_s (yrs)	Peak time t_p (yrs)	Ascent time T_a (yrs)	Descent time T_d (yrs)	Length T_{cy} (yrs)	S_{max}	S_{min}	A_w (days)	$[T_{cy}]_{predicted}$ (yrs)	Error τ_{error} (yrs)
1	1755.13	1761.46	6.33	4.92	11.25	86.5	8.4	–	–	–
2	1766.38	1769.71	3.33	5.75	9.08	115.8	11.2	–	–	–
3	1775.46	1778.38	2.92	6.33	9.25	158.5	7.2	–	–	–
4	1784.71	1788.13	3.42	10.17	13.58	141.2	9.5	–	–	–
5	1798.29	1805.13	6.83	5.00	11.83	49.2	3.2	–	–	–
6	1810.13	1816.38	6.25	6.83	13.08	48.7	0.0	–	–	–
7	1823.21	1829.88	6.67	4.00	10.67	71.5	0.1	–	–	–
8	1833.88	1837.21	3.33	6.33	9.67	146.9	7.3	–	–	–
9	1843.54	1848.13	4.58	7.83	12.42	131.9	10.6	–	–	–
10	1855.96	1860.13	4.17	7.08	11.25	98.0	3.2	4.9	–	–
11	1867.21	1870.63	3.42	8.33	11.75	140.3	5.2	5.5	–	–
12	1878.96	1883.96	5.00	6.17	11.17	74.6	2.2	3.6	11.56	0.39
13	1890.13	1894.04	3.92	8.00	11.92	87.9	5.0	3.4	11.48	−0.43
14	1902.04	1906.13	4.08	7.33	11.42	64.2	2.7	3.6	10.93	−0.49
15	1913.46	1917.63	4.17	5.92	10.08	105.4	1.5	4.2	9.62	−0.46
16	1923.54	1928.29	4.75	5.42	10.17	78.1	5.6	3.3	10.01	−0.16
17	1933.71	1937.29	3.58	6.83	10.42	119.2	3.5	5.1	10.77	0.35
18	1944.13	1947.38	3.25	6.92	10.17	151.8	7.7	5.3	10.34	0.17
19	1954.29	1958.21	3.92	6.58	10.50	201.3	3.4	4.3	11.20	0.70
20	1964.79	1968.88	4.08	7.33	11.42	110.6	9.6	3.6	11.09	−0.32
21	1976.21	1979.96	3.75	6.75	10.50	164.5	12.2	5.9	10.63	0.13
22	1986.71	1989.54	2.83	6.83	9.67	158.5	12.3	5.6	10.01	0.34
23	1996.38	2000.29	3.92	8.58	12.50	120.8	8.0	4.2	12.27	−0.23
24	2008.88	–	5.42	–	–	81.9	1.7	4.1	**11.01**	–
25	–	–	–	–	–	–	–	–	**10.52**	–
26	–	–	–	–	–	–	–	–	**11.91**	–

Table 2 Solar cycle characteristics such as start time (t_s), peak time (t_p), ascent time (T_a), descent time (T_d), length of SC (T_{cy}), peak sunspot number (S_{max}) and minimum sunspot number (S_{min}) for the Version 2 sunspot series. The autocorrelation width (A_w), the SC length predicted using the model equation, and the error (τ_{error}) in the observed and predicted T_{cy} are given in the last three columns.

SC No.	Start time t_s (yrs)	Peak time t_p (yrs)	Ascent time T_a (yrs)	Descent time T_d (yrs)	Length T_{cy} (yrs)	S_{max}	S_{min}	A_w (days)	$[T_{cy}]_{predicted}$ (yrs)	Error τ_{error} (yrs)
1	1755.12	1761.46	6.33	5.00	11.33	144.1	14.0	–	–	–
2	1766.46	1769.71	3.25	5.75	9.00	193.0	18.6	–	–	–
3	1775.46	1778.37	2.92	6.34	9.25	264.3	12.0	–	–	–
4	1784.71	1788.12	3.42	10.16	13.58	235.3	15.9	–	–	–
5	1798.29	1805.12	6.84	5.08	11.92	82.0	5.3	–	–	–
6	1810.20	1816.37	6.17	6.83	13.00	81.2	0.0	–	–	–
7	1823.20	1829.87	6.67	4.00	10.67	119.2	0.2	–	–	–
8	1833.87	1837.20	3.33	6.33	9.66	244.9	12.2	–	–	–
9	1843.54	1848.12	4.59	7.83	12.42	219.9	17.6	–	–	–
10	1855.96	1860.12	4.17	7.08	11.25	186.2	6.0	4.8	–	–
11	1867.20	1870.62	3.42	8.34	11.75	234.0	9.9	5.5	–	–
12	1878.96	1883.96	5.00	6.25	11.25	124.4	3.7	3.6	11.55	0.61
13	1890.20	1894.04	3.84	8.00	11.84	146.5	8.3	3.3	11.61	−0.19
14	1902.04	1906.12	4.08	7.42	11.50	107.1	4.5	3.6	11.01	−0.55
15	1913.54	1917.62	4.09	5.92	10.00	175.7	2.5	4.1	9.50	−0.35
16	1923.54	1928.29	4.75	5.42	10.17	130.2	9.4	3.3	10.09	−0.01
17	1933.71	1937.29	3.58	6.84	10.42	198.6	5.8	5.1	10.67	0.15
18	1944.12	1947.37	3.25	6.92	10.16	218.7	12.9	4.8	10.42	0.26
19	1954.29	1958.20	3.92	6.59	10.50	285.0	5.1	4.4	11.31	0.77
20	1964.79	1968.87	4.08	7.33	11.42	156.6	14.3	3.6	10.63	−0.88
21	1976.21	1979.96	3.75	6.75	10.50	232.9	17.8	5.8	10.84	0.30
22	1986.71	1989.87	3.17	6.50	9.67	212.5	13.5	5.2	10.09	0.36
23	1996.37	2001.87	5.50	7.08	12.59	180.3	11.2	4.2	12.28	−0.47
24	2008.96	2014.29	5.33	–	–	116.4	2.2	3.9	**11.01**	–
25	–	–	–	–	–	–	–	–	**12.20**	–
26	–	–	–	–	–	–	–	–	**11.68**	–

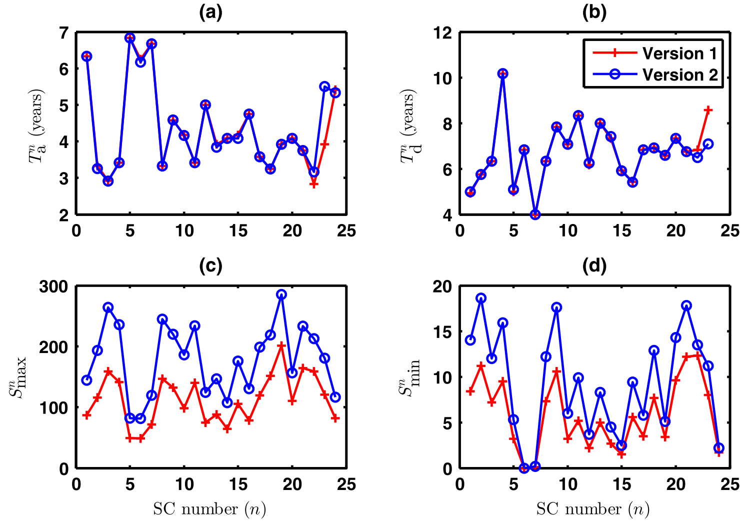

Figure 2 Variation in SC characteristics: (**a**) ascent time, (**b**) descent time, (**c**) solar maximum, and (**d**) solar minimum estimated from the monthly SSN of Version 1 (*red*) and Version 2 (*blue*) for SCs 1 – 24.

a given phase is represented by $\langle S_a \rangle$. It may be noted that we estimated the autocorrelation function only for Phase 2 of each SC and used this in the present model. In Figure 3, as an example, we show the signal $S_a - \langle S_a \rangle$ during Phase 2 of i) SC 15 and ii) SC 22 for Version 1 (red) and Version 2 (blue). The corresponding autocorrelation functions are shown in Figures 3c and 3d as a function of time lag (ζ) in days. Each autocorrelation function is fitted with a fifth-order polynomial. Then, the width of an autocorrelation function (A_w), defined as the lag where it falls to 0.65, was estimated for each signal. The time lags in the autocorrelation functions are discrete, whereas the width of the autocorrelation function may not always be discrete. In order to obtain the appropriate information on the width of the autocorrelation function, we fitted the autocorrelation function with a fifth-order polynomial and recomputed the values of the autocorrelation with a time lag of 0.1 days. For SCs 15 and 22, the widths of the autocorrelation functions are found to be 4.2 days and 5.6 days (4.1 days and 5.2 days) for the Version 1 (Version 2) sunspot series, respectively. The estimates of A_w for SCs 10 – 24 are given in the third last columns of Tables 1 and 2.

We found that the autocorrelation width A_w^n during Phase 2 is highly correlated with i) the length of SC $n+2$ (*i.e.* T_{cy}^{n+2}), and ii) the ascent time of SC n (*i.e.* T_a^n), resulting in correlation coefficients of 0.79 and −0.67 (0.77 and −0.57) for Version 1 (Version 2), respectively. We defined a new parameter $T_{cy}^{n+2} - T_a^n$ and termed it modified length, which possesses a significantly higher correlation with A_w^n. The plot of the modified length $T_{cy}^{n+2} - T_a^n$ as a function of A_w^n for SCs 10 – 21 (*i.e.* $n = 10-21$) is shown in Figure 4 for i) Version 1 and ii) Version 2. The correlation coefficient between the modified length and the width of the autocorrelation is found to be 0.93 and 0.91 for Versions 1 and 2, respectively. The linear equations obtained using the least-squares fit for Versions 1 and 2 are

$$\text{Version 1:} \quad T_{cy}^{n+2} - T_a^n = 1.13 A_w^n + 1.87, \tag{1}$$

$$\text{Version 2:} \quad T_{cy}^{n+2} - T_a^n = 1.15 A_w^n + 1.88. \tag{2}$$

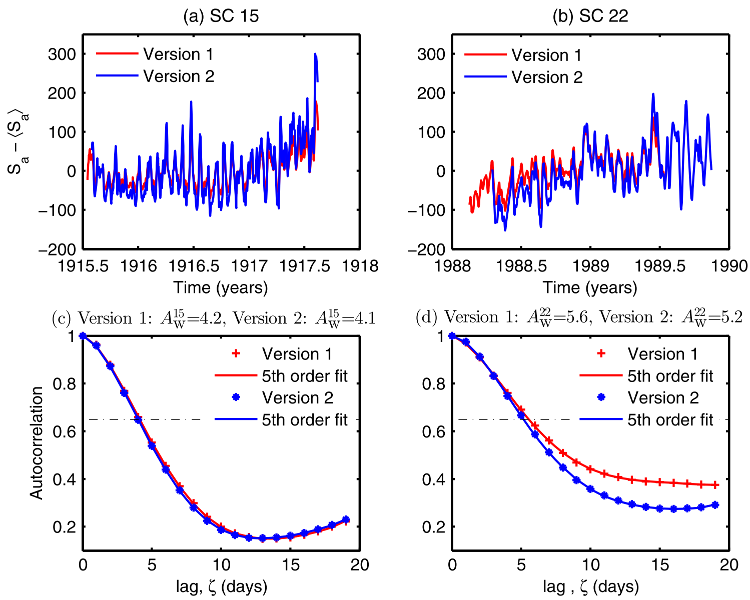

Figure 3 Variation in $S_a - \langle S_a \rangle$ as a function of time during Phase 2 of the ascent stage of (**a**) SC 15 and (**b**) SC 22 for Version 1 (*red*) and Version 2 (*blue*). The corresponding autocorrelation functions are shown in panels (**c**) and (**d**). The values of the width of the autocorrelation functions are given in each *subplot*. The *horizontal black dash-dotted line* shows the limit of 0.65, which is used to compute the width of the autocorrelation function.

Figure 4 Modified length $T_{\mathrm{cy}}^{n+2} - T_{\mathrm{a}}^{n}$ as a function of the width of the autocorrelation function A_{W}^{n} of SCs 10 – 21 for (**a**) Version 1 and (**b**) Version 2. The linear least-squares fitted equations and the correlation coefficients are given in the *subplots*.

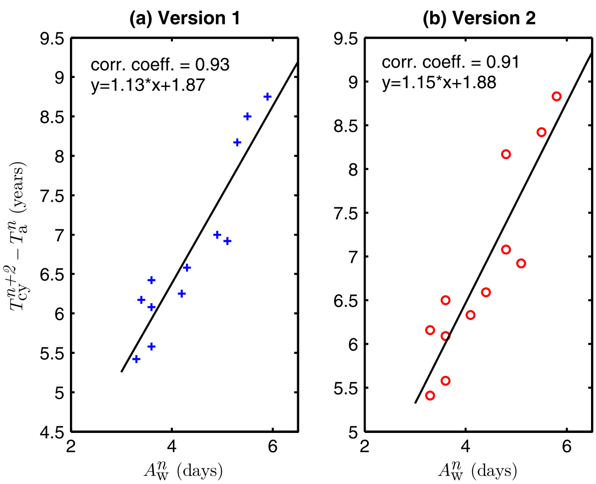

Equations 1 and 2 can be used to predict the length of SC $n+2$ when the width of the autocorrelation function during Phase 2 and the ascent time of SC n are known. From Equations 1 and 2, we estimated T_{cy} for SCs 12 – 23 using the values of A_{w} and T_{a} for SCs 10 – 21. These length estimates are listed in Tables 1 and 2 for the Version 1 and Version 2 sunspot data series, respectively. The difference between the predicted and the observed length of the SCs is represented by τ_{error}, and it is listed in Tables 1 and 2 for SCs 12 – 23. It

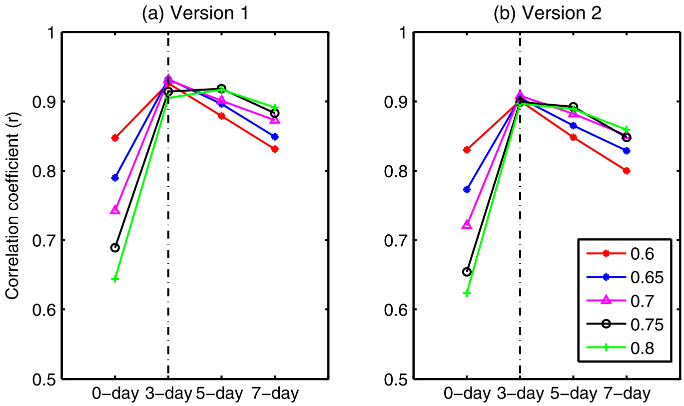

Figure 5 Correlation coefficient between model parameters as a function of the size of the smoothing window applied to the sunspot series of (**a**) Version 1 and (**b**) Version 2. Different *color curves* correspond to different limits C_l considered while estimating the width of the autocorrelation function. The maximum correlation coefficient for the model parameters is found for the three-day smoothing with $C_l = 0.6 - 0.7$.

is evident that the absolute error ($|\tau_{\text{error}}|$) between the observed and the predicted length of the SCs lies between $0.13 - 0.7$ years ($0.08 - 0.81$ years) with a standard rms deviation and $\sigma_{\text{prediction}}$ of 0.38 years (0.44 years) for Version 1 (Version 2). As the parameters used in the model possess higher correlation with smaller standard errors in the prediction, this can be used to predict the length of upcoming SCs. The advantage of this model is that the forecast of the length of two SCs, *i.e.* $n + 1$ and $n + 2$, is available at the time of the peak of SC n.

It may be noted that we used the information in the autocorrelation function of the sunspot numbers only during Phase 2 of the ascending stage of a given SC because the widths of the autocorrelation function during other phases are not found to be well correlated with the parameter that we plan to model in the present study. Second, in this model we specifically chose i) a smoothing function of three days, which was applied to the sunspot series, and ii) the widths of the autocorrelation function were defined by imposing the limit (C_l) of 0.65. The parameter C_l is defined as the value of the autocorrelation used to obtain the width of the autocorrelation function. Here, the question is why we chose these parameters for the proposed model, and if we were to change these parameters, how that would affect the model output. To address these questions, we tested our model with no smoothing, with three-day smoothing, with five-day smoothing, and with seven-day smoothing. We also changed the limit C_l to 0.6, 0.65, 0.7, 0.75, and 0.8, to obtain the width of the autocorrelation function. A similar exercise was carried out, and the correlation coefficients between model parameters (as described in previous paragraphs) were obtained for each combination of smoothing function and the limit C_l. The plot of the correlation coefficient as a function of smoothing window for different values of C_l is shown in Figure 5 for Version 1 and Version 2 sunspot data. It is noted that the maximum correlation between the model parameters is encountered for the three-day smoothing and the limit C_l =0.65. When we used a somewhat wider window size for the smoothing function, *i.e.* five and seven days, the correlation coefficient started to decrease. This is expected because as we increase the size of the smoothing window, the information on short timescale variations will be averaged out. Furthermore, for a three-day smoothing window, the correlation coefficients are 0.901, 0.905, and 0.908 (0.926, 0.932, and 0.931) for the limit $C_l = 0.6$, 0.65, and 0.7, respectively for the Version 1 (Version 2) sunspot series. This indicates that the correlation coefficients are varying less significantly when C_l is selected to lie between $0.6 - 0.7$ to estimate the width of the

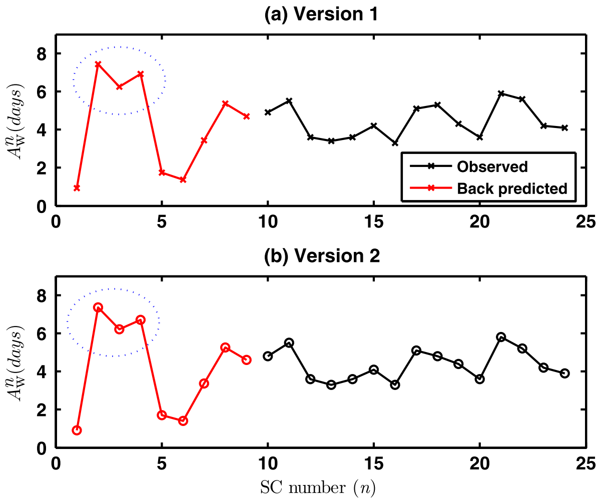

Figure 6 Back-predicted (*red*) and estimated widths of the autocorrelation function for (**a**) Version 1 and (**b**) Version 2 shown as a function of SC number.

autocorrelation function. Thus in the proposed model, we took the three-day smoothing and the limit of 0.65 to define the width of the autocorrelation function. The autocorrelation is simply a serial correlation between two signals. Taking very low values (< 0.6) to compute the autocorrelation width will be statistically insignificant because while doing so, we basically move toward the regime of lower correlations. We took 0.65 as the limit to define the width of the autocorrelation function, which means that the 65% of the variations between the signal $f(t)$ and the time-shifted signal $(f(t-\zeta))$ match well at lag $\zeta = A_\mathrm{w}$.

Using Equations 1 and 2, we computed the length of SCs 24, 25, and 26 as the information on T_a and A_w were available only for SCs 22 – 24. The proposed model gives a forecast of 11.01, 10.52, and 11.91 years (11.01, 12.20, and 11.68 years) for SCs 24, 25, and 26, respectively, for the Version 1 (Version 2) sunspot series. The standard error in the range of $\pm 0.38 - 0.44$ years is expected in the predicted lengths of SCs. SC 24 is initiated at 2008.88 (2008.96) for Version 1 (Version 2), thus based on the present prediction of T_{cy}^{24}, it is likely to end in November 2019 (December 2019).

It may be noted that we were able to compute A_w only for SCs 10 – 24 as daily sunspot data were available for this period. A careful examination of Equations 1 and 2 indicates that we can estimate the width of the autocorrelation function for SCs 1 – 9 by rewriting these equations as follows:

$$\text{Version 1:}\quad A_\mathrm{w}^n = (T_\mathrm{cy}^{n+2} - T_\mathrm{a}^n - 1.87)/1.13, \tag{3}$$

$$\text{Version 2:}\quad A_\mathrm{w}^n = (T_\mathrm{cy}^{n+2} - T_\mathrm{a}^n - 1.88)/1.15. \tag{4}$$

Using Equations 3 and 4, we back-predicted the autocorrelation widths of SCs 1 – 9 for Versions 1 and 2. These back-predicted (red) and estimated (black) values of A_w^n are shown in Figure 6 for i) Version 1 and ii) Version 2. It is noted that the period of the Dalton minimum (SCs 5 – 7) is associated with longer autocorrelation widths. This is an interesting feature and hints at the presence of a different dynamo process during these periods. The model results are discussed in the next section to achieve further insights into the present study.

3. Discussion and Conclusions

We have retrieved information on the width of the autocorrelation function during the second half of the ascending phase (termed Phase 2) for each SC using the daily international sunspot series (Versions 1 and 2). The estimated widths of the autocorrelation function A_{w} in this phase are found to vary with the SCs. With our model equation, the back-predicted values of A_{w} for SCs $1-9$ suggest that the widths of the autocorrelation function become longer during periods of weaker solar activity, such as the Dalton minimum. The question is why the width of the autocorrelation function varies with SC. For G- and K-type stars, Böhm-Vitense (2007) showed that the activity period (cycle length) of a star is proportional to its rotation period. However, this dependence follows different linear trends for active and inactive stars. It is attributed to differences in the internal dynamo processes that are operative during active and inactive phases of these stars. It may be noted that we computed the autocorrelation functions using observations of sunspot numbers. These sunspots appear at high latitude in their initial phase of activity and then slowly move toward the equatorial belt during the time close to peak activity. It is known that the latitudes of the Sun rotate at different rates (Spence *et al.*, 1993). For example, the rotation period at the solar poles is ≈ 40 days, and at the solar equator, it is ≈ 27 days (Noyes, 1982). In addition, these rotation periods are a function of solar activity and the phase of a cycle (Aini Kambry and Nishikawa, 1990). Thus, a variation in the width of the autocorrelation function with SCs is expected.

Another question is what a larger A_{w} during the Dalton minimum signifies. For any time series, the autocorrelation measures the relation of the present observation (*i.e.* at time t) with past or future observations (*i.e.* at time $t \mp \zeta$) for different time lags ζ. It is also treated as a measure of the persistence (repeating behavior). The autocorrelation function falls to a value lower than 0.5 within a lag of less than ten days for SCs $10-24$. The slow change in the autocorrelation indicates that the observed feature is sustained for a longer time with less variability. In long-memory processes, the decay of the autocorrelation function for a time series can be expressed as a power law $\propto \zeta^{-\alpha}$, where α is the power-law index. For such systems, the Hurst exponent H is given by $1 - \alpha/2$. The Hurst exponent varies between $0-1$, and it is used to give information about memory in a given time series. If $0 \leq H < 0.5$ ($0.5 < H \leq 1$), then the time series possesses less (more) persistence (Ruzmaikin, Feynman, and Robinson, 1994; Oliver and Ballester, 1996; Kilcik *et al.*, 2009). In other words, systems with greater persistence will tend to have shallower slopes (*i.e.* $\alpha = 0-1$) in their autocorrelation function.

In view of this discussion, our analysis suggests that the dynamo processes that are operative during weak solar activity have a tendency to move toward the persistence behavior. We confirmed this hypothesis by estimating the Hurst exponent H by a rescaled range analysis (Gilmore *et al.*, 2002). The exponent is found to vary between $0.73-0.88$ for the Version 1 and Version 2 sunspot series for Phase 2. We noted that the Hurst exponent is directly proportional to the width of the autocorrelation function, such that it gives a correlation coefficient of 0.88 (0.89) for Version 1 (Version 2). In recent studies, the values of the Shannon entropy, a measure of inherent randomness in the system, have been found to be lower during the period of the Dalton minimum (Kakad, Kakad, and Ramesh, 2015, 2017). This is in agreement with the persistence behavior of solar activity during the Dalton minimum.

Recently, Kakad, Kakad, and Ramesh (2015) proposed a new method for predicting the descent time, which suggests that SC 24 would end around February 2021. This prediction suggests that the end of SC 24 will be nearly 13 months later than the value given by the present model. An onset of SC 25 close to the end of 2019 has been suggested by McIntosh *et al.* (2014). Other recent predictions are also available at http://www.huffingtonpost.

com/dr-sten-odenwald/ and http://www.aurorab orealispage.net/solarmax.html, which suggests that SC 24 is likely to end around 2019 – 2020. This is in agreement with our model predictions.

In conclusion, we have developed a new model to predict the length of upcoming SCs. With this model, the cycle length can be forecast for two upcoming SCs. The model was validated using Version 1 and Version 2 sunspot series. The standard error in the prediction of the SC length is 0.38 years and 0.44 years for the Version 1 and Version 2 data, respectively. The model gives a forecast of 11.01, 10.52, and 11.91 years (11.01, 12.20, and 11.68 years) for SCs 24, 25, and 26, respectively, for the Version 1 (Version 2) sunspot series. It suggests that SC 24 will be of normal length, but SCs 25 and 26 are likely to have lengths greater than the average length of 11 years. The widely known amplitude-width relation of SCs suggests that the solar maximum of SC n is inversely correlated with the length of SC $n-1$. As the predicted lengths of SCs 25 and 26 are somewhat greater than the average length of all SCs, the upcoming SCs 26 and 27 are likely to have weaker solar activity, which is in agreement with recent studies (Gkana and Zachilas, 2016; Zachilas and Gkana, 2015). The present study also indicates a tendency of a persistency in the solar dynamo process that is operative during periods of weak solar activity.

Acknowledgements We thank the SIDC and SILSO teams for the daily and monthly international sunspot data. The revisions of the manuscript were carried out at the Research Institute of Sustainable Humanosphere, Kyoto University, Japan.

Disclosure of Potential Conflicts of Interest The authors declare that they have no conflicts of interest.

References

Aini Kambry, M., Nishikawa, J.: 1990, Solar differential rotation derived from sunspot observations. *Solar Phys.* **126**(1), 89. DOI.

Böhm-Vitense, E.: 2007, Chromospheric activity in G and K main-sequence stars, and what it tells us about stellar dynamos. *Astrophys. J.* **657**, 486. DOI. ADS.

Clette, F., Svalgaard, L., Vaquero, J.M., Cliver, E.W.: 2015, In: Balogh, A., Hudson, H., Petrovay, K., von Steiger, R. (eds.) *Revisiting the Sunspot Number*, Springer, New York, 35. DOI.

Clette, F., Cliver, E.W., Lefèvre, L., Svalgaard, L., Vaquero, J.M., Leibacher, J.W.: 2016a, Preface to topical issue: Recalibration of the sunspot number. *Solar Phys.* **291**(9), 2479. DOI.

Clette, F., Lefèvre, L., Cagnotti, M., Cortesi, S., Bulling, A.: 2016b, The revised Brussels–Locarno sunspot number (1981 – 2015). *Solar Phys.* **291**(9), 2733. DOI.

de Toma, G., Gibson, S., Emery, B., Arge, C.: 2010, The minimum between cycle 23 and 24: Is sunspot number the whole story? In: *SOHO-23: Understanding a Peculiar Solar Minimum* **428**, 217. ADS.

Dikpati, M., Gilman, P.A.: 2008, Global solar dynamo models: Simulations and predictions. *J. Astrophys. Astron.* **29**(1-2), 29. DOI.

Emmert, J., Lean, J., Picone, J.: 2010, Record-low thermospheric density during the 2008 solar minimum. *Geophys. Res. Lett.* **37**(12), L12102. DOI.

Ermolli, I., Matthes, K., Dudok de Wit, T., Krivova, N.A., Tourpali, K., Weber, M., Unruh, Y.C., Gray, L., Langematz, U., Pilewskie, P., *et al.*: 2013, Recent variability of the solar spectral irradiance and its impact on climate modelling. *Atmos. Chem. Phys.* **13**(8), 3945. DOI.

Feynman, J.: 1982, Geomagnetic and solar wind cycles, 1900 – 1975. *J. Geophys. Res.* **87**(A8), 6153. DOI.

Gilmore, M., Yu, C.X., Rhodes, T.L., Peebles, W.A.: 2002, Investigation of rescaled range analysis, the hurst exponent, and long-time correlations in plasma turbulence. *Phys. Plasmas* **9**(4), 1312. DOI.

Gkana, A., Zachilas, L.: 2016, Re-evaluation of predictive models in light of new data: Sunspot number version 2.0. *Solar Phys.* **291**, 2457. DOI.

Hajra, R., Tsurutani, B.T., Echer, E., Gonzalez, W.D.: 2014, Relativistic electron acceleration during high-intensity, long-duration, continuous ae activity (hildcaa) events: Solar cycle phase dependences. *Geophys. Res. Lett.* **41**(6), 1876. DOI.

Hao, Y., Shi, H., Xiao, Z., Zhang, D.: 2014, Weak ionization of the global ionosphere in solar cycle 24. In: *Ann. Geophys.* **32**, 809. DOI.

Hathaway, D.H.: 2010, The solar cycle. *Living Rev. Solar Phys.* **7**(1), 1. DOI.
Hathaway, D.H., Wilson, R.M.: 2006, Geomagnetic activity indicates large amplitude for sunspot cycle 24. *Geophys. Res. Lett.* **33**(18), L18101. DOI.
Hathaway, D.H., Wilson, R.M., Reichmann, E.J.: 2002, Group sunspot numbers: Sunspot cycle characteristics. *Solar Phys.* **211**(1), 357. DOI.
Kakad, B.: 2011, A new method for prediction of peak sunspot number and ascent time of the solar cycle. *Solar Phys.* **270**(1), 393. DOI.
Kakad, B., Kakad, A., Ramesh, D.S.: 2015, A new method for forecasting the solar cycle descent time. *J. Space Weather Space Clim.* **5**, A29. DOI. ADS.
Kakad, B., Kakad, A., Ramesh, D.S.: 2017, Shannon entropy-based prediction of solar cycle 25. *Solar Phys.* **292**, 95. DOI. ADS.
Kane, R.P.: 2008, Prediction of solar cycle maximum using solar cycle lengths. *Solar Phys.* **248**(1), 203. DOI.
Kilcik, A., Anderson, C.N.K., Rozelot, J.P., Ye, H., Sugihara, G., Ozguc, A.: 2009, Nonlinear prediction of solar cycle 24. *Astrophys. J.* **693**(2), 1173. DOI.
McComas, D., Ebert, R., Elliott, H., Goldstein, B., Gosling, J., Schwadron, N., Skoug, R.: 2008, Weaker solar wind from the polar coronal holes and the whole sun. *Geophys. Res. Lett.* **35**(18), L18103. DOI.
McIntosh, S.W., Wang, X., Leamon, R.J., Davey, A.R., Howe, R., Krista, L.D., Malanushenko, A.V., Markel, R.S., Cirtain, J.W., Gurman, J.B., Pesnell, W.D., Thompson, M.J.: 2014, Deciphering solar magnetic activity, I: On the relationship between the sunspot cycle and the evolution of small magnetic features. *Astrophys. J.* **792**(1), 12. DOI.
Muñoz-Jaramillo, A., Dasi-Espuig, M., Balmaceda, L.A., DeLuca, E.E.: 2013, Solar cycle propagation, memory, and prediction: insights from a century of magnetic proxies. *Astrophys. J. Lett.* **767**(2), L25. DOI.
Noyes, R.W.: 1982, *The Sun, Our Star*. ADS.
Ohl, A.: 1966, Wolf's number prediction for the maximum of the cycle 20. *Soln. Dannye* **12**, 84.
Oliver, R., Ballester, J.L.: 1996, Rescaled range analysis of the asymmetry of solar activity. *Solar Phys.* **169**(1), 215. DOI.
Pesnell, W.D.: 2008, Predictions of solar cycle 24. *Solar Phys.* **252**(1), 209. DOI.
Pesnell, W.D.: 2016, Predictions of solar cycle 24: How are we doing? *Space Weather* **14**(1), 10. DOI.
Ruzmaikin, A., Feynman, J., Robinson, P.: 1994, Long-term persistence of solar activity. *Solar Phys.* **152**(1), 313. DOI.
Solomon, S.C., Qian, L., Burns, A.G.: 2013, The anomalous ionosphere between solar cycles 23 and 24. *J. Geophys. Res.* **118**(10), 6524. DOI.
Spence, P., Walker, E.N., Halls, B., Roberton, L.: 1993, Periodicities in the relative sunspot number during sunspot maximum of solar cycle 22. *J. Br. Astron. Assoc.* **103**, 115. ADS.
Svalgaard, L., Kamide, Y.: 2012, Asymmetric solar polar field reversals. *Astrophys. J.* **763**(1), 23. DOI.
Thompson, R.: 1993, A technique for predicting the amplitude of the solar cycle. *Solar Phys.* **148**(2), 383. DOI.
Usoskin, I.G., Solanki, S., Kovaltsov, G.: 2011, Grand minima of solar activity during the last millennia. *Proc. Int. Astron. Union* **7**(S286), 372. DOI.
Waldmeier, M.: 1935. *Astron. Mitt. (Zür.)* **14**, 105.
Waldmeier, M.: 1939. *Astron. Mitt. (Zür.)* **14**, 439.
Wilson, R.M.: 1990, On the level of skill in predicting maximum sunspot number: A comparative study of single variate and bivariate precursor techniques. *Solar Phys.* **125**(1), 143. DOI.
Zachilas, L., Gkana, A.: 2015, On the verge of a grand solar minimum: A second Maunder minimum? *Solar Phys.* **290**(5), 1457. DOI.